Talanta 132 (2015) 278–284

Contents lists available at ScienceDirect

Talanta

journal homepage: www.elsevier.com/locate/talanta

Highly selective visual monitoring of hazardous fluoride ion in aqueous media using thiobarbituric-capped gold nanoparticles

Jyoti Boken [a], Sheenam Thatai [b], Parul Khurana [b], Surendra Prasad [c,*], Dinesh Kumar [b,**]

[a] Department of Physics, Banasthali University, Banasthali-304022, Rajasthan, India
[b] Department of Chemistry, Banasthali University, Banasthali-304022, Rajasthan, India
[c] School of Biological and Chemical Sciences, Faculty of Science, Technology and Environment, The University of the South Pacific, Private Mail Bag, Suva, Fiji

ARTICLE INFO

Article history:
Received 17 June 2014
Received in revised form
14 August 2014
Accepted 14 August 2014
Available online 16 September 2014

Keywords:
Gold nanoparticles
2-Thiobarbituric acid
Fluoride ion sensor
Naked-eye detection
Colorimetric

ABSTRACT

The rapid, selective and sensitive measurement and monitoring of hazardous materials as analytes are the central themes in the development of any successful analytical technique. With this aim, we have synthesized the thiobarbituric-capped gold nanoparticles (TBA-capped Au NPs) involving chemical reduction of $HAuCl_4$ using 2-thiobarbituric acid (TBA) as a reducing and capping agent. The morphology of the TBA-capped Au NPs was confirmed using transmission electron microscope images. For the first time this article reports that the developed TAB-capped Au NPs displays selective, ultrafast and sensitive colorimetric detection of fluoride ion in aqueous samples. The detection of fluoride ion was confirmed by the disappearance of the localized surface plasmon resonance (LSPR) band at 554 nm using UV-vis spectroscopy. The interaction of F^- with TBA-capped Au NPs in aqueous solution has also been confirmed by Raman and FTIR spectroscopy. One of the most exciting accomplishments is the visual detection limit for fluoride ion has been found to be 10 mM at commonly acceptable water pH range 7–8. The whole detection procedure takes not more than 40 s with excellent selectivity providing sample throughput of more than 60 per hour.

1. Introduction

Metal nanoparticles such as gold nanoparticles (Au NPs) have attracted much attention with wide applications in highly sensitive chemical sensors due to their optical and electrical properties [1,2]. These properties of Au NPs are precisely determined by their dimension [2], shape [3], composition of materials [4,5], surrounding media [6] and relative distance between the particles [7–9]. Therefore, NPs show the intense plasmon resonance band in the visible region [10,11] which is exquisitely sensitive to their aggregation states [12,13].

Fluoride is commonly added to drinking water and toothpaste because of their beneficial effects on dental health. The deficiency of fluoride causes poor dental health and osteoporosis [14,15], while over exposure to fluoride ion causes fluorosis and urolithiasis [16–19]. Even small excess amount of fluoride consumed from tap water can damage bones, teeth, brain, disrupt thyroid function, lower intelligence quotient and/or cause cancer [14–19]. Thus, the Environmental Protection Agency (EPA) has set a maximum level of fluoride ion in water as 1 ppm and that over 2 ppm is considered a health risk [20]. Therefore, the accuracy in detection and determination of fluoride ion in aqueous samples is an extremely important aspect in the public interest. Recently, the colorimetric sensors or nanoprobes have been widely used for selective and sensitive detection for several analytes including alkali metal ions [21,22], heavy metal ions [23,24], oxo anions [25–27], fluoride ion [24,28–37], iodide ion [38], DNA and biomolecules [39–42], hydrogen peroxide [43], organophosphates [44], etc. However, there is still need to develop methods for sensing of fluoride ion due to its various applications.

Fluoride has unique properties compared to other elements as a result of its relative by small size and highest electronegativity. Thus, a number of compounds that are able to bind fluoride ion with high affinity and selectivity have been reported, but only a few reports are available in the literature for fluoride ion probes that utilize the unique optical properties of Au NPs [30,35]. However, the sensitivity and selectivity of this probe were poor compared to the properties of the other probes based on fluorescence and colorimetric probes [35]. The disadvantage on nanoprobes development is that the limited Au NPs are acquirable. In most cases Au NPs have been synthesized by citrate, which dispersed in an aqueous solution through the ionic repulsion of the surface-adsorbed ions. In the presence of electrolytes, due to the charge shielding, the ionic stabilized NPs undergo uncontrolled aggregation. The stabilized Au NPs are protected with non-ionic hydrophilic molecules, but the

* Corresponding author. Tel.: +679 3232416; fax: +679 2321512.
** Corresponding author. Tel.: +91 9928108023; fax: +91 1438 228365.
E-mail addresses: prasad_su@usp.ac.fj (S. Prasad), dschoudhary2002@yahoo.com (D. Kumar).

http://dx.doi.org/10.1016/j.talanta.2014.08.043
0039-9140/

thick protecting layers preventing the core metals to be close together, which are responsible for the change in color in the solution [45]. Therefore, it is essential to develop Au NPs protected with a monolayer of hydrophilic molecules.

Mostly sensors are fluorescent sensors containing quinoline [46], coumarin [47], anthracene [48], fluorescein fluorophores [49–55], pyrroles [56], quinoxalies [57–59] and azophenols [60,61]. Although, fluorescent sensors are widely used in biological studies, they usually require complicated synthesis involving various reaction condition and expensive chemicals. On the other hand, detection method used often required expensive equipment. Thus, it is of great interest to develop new chemical sensors which use easily synthesized chemicals and possesses good selectively and high sensitivity. Fluoride ion sensors are in great demand due to the involvement of fluoride in a variety of environmental issues and healthcare [36,62]. Therefore, a variety of fluoride sensors have been developed [24,28–37]. A selective and sensitive chemosensor that makes use of transition between Au NPs agglomeration states to develop a signal in the presence of fluoride ion is an attractive approach to fabricate fast usability fluoride ion probes [30,35]. With the aim to obtain more sensitive and selective chemosensors, an increasing number of papers have recently appeared, in which the chemosensor have been anchored to different supports [49]. In addition, the application of Au NPs as colorimetric sensors have usually been based on detecting the peak shifts in surface plasmon resonance (SPR) either due to the change in the dielectric constant around the NPs as a result of analyte molecule adsorption or to the analyte induced agglomeration of the NPs [13]. Both effects have provided the selectivity in detection by the functionalized capping agents, highlighting the importance of the synthesis by chemical reduction methods and their stabilization of NPs for use a solution based sensors [63].

In continuation of our interest on developing analytical methods for fluoride removal [15,16] and development of nanosensor for the detection of cations using Au nano-rods [17], and with continuous report on hazardous fluoride contamination in drinking water in rural habitations of Central Rajasthan, India [16], we continued our work towards the development of novel rapid, selective and sensitive method for visual detection and monitoring of hazardous fluoride ion. Thus, herein we introduce an easy, simple and quantitative preparation of the modified Au NPs with 2-thiobarbituric acid (TBA) where UV–vis absorption study has demonstrated that the fluoride selective aggregation is associated with dramatic color change in aqueous solution which leads to rapid, selective and sensitive method for visual detection and monitoring of hazardous fluoride ion. The different agglomeration states of Au NPs produce a different color in the solution. This study has also demonstrated that TBA is a potential candidate to devise the reliable ultrafast colorimetric sensor for the naked-eye visualization of fluoride ion detection at trace level.

2. Materials and methods

2.1. Chemicals

Tetrachloroauric acid and 2-thiobarbituric acid purchased from Sigma-Aldrich (USA) were used as received without any further purification. The regents for all anions (sodium fluoride, potassium

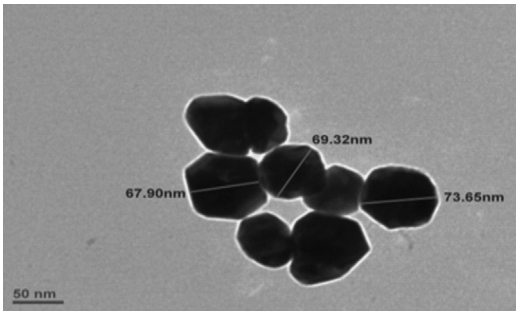

Fig. 2. TEM image of 2-thiobarbituric-capped gold nanoparticles.

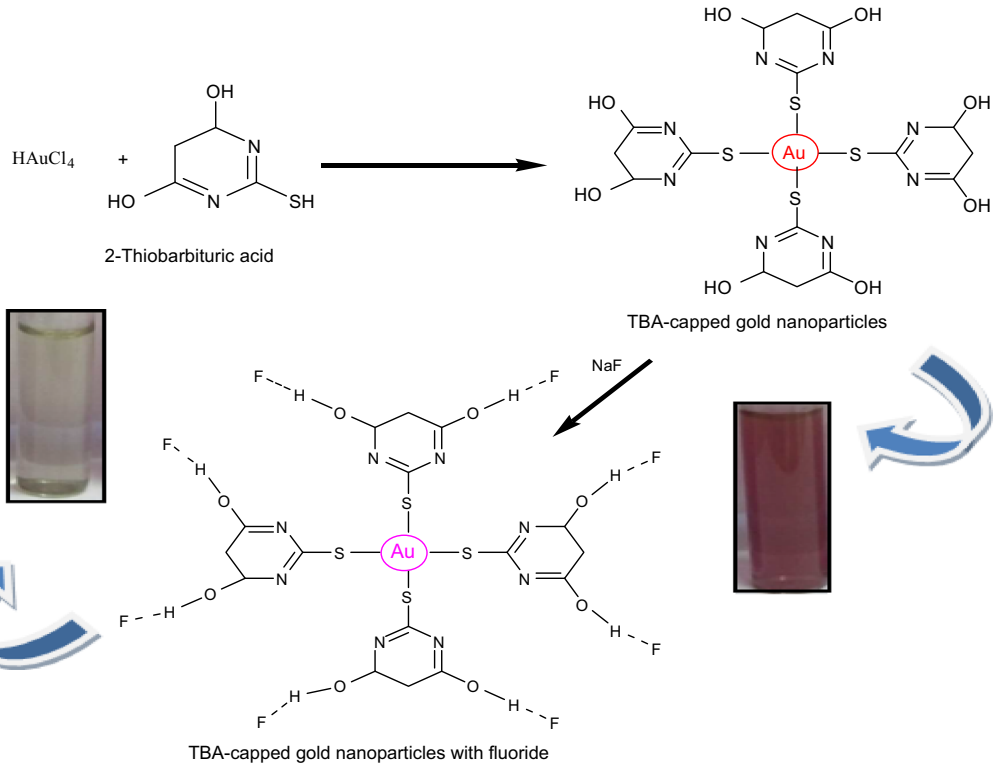

Fig. 1. A schematic representation for fabrication of 2-thiobarbituric capped gold nanoparticles and sensing of fluoride ions.

bromide, sodium chloride, potassium iodide, potassium carbonate, acetic acid, sodium nitrate, potassium dihydrogen phosphate) were purchased from E. Merck Ltd, Mumbai, India. All the solutions were freshly prepared for the synthesis of nanoparticles. Distilled water passed through a Millipore system (resistivity 18 MΩ. cm) was used in the preparation of all the solutions and throughout the experiments. All glassware used were first rinsed with aqua regia and then thoroughly washed with distilled water followed by Millipore water.

2.2. Synthesis of TBA-capped Au NPs

Thiobarbituric-capped Au NPs was synthesized by a wet chemical reduction method where TBA acts as reducing agent as well as capping agent [64]. In synthesis of TBA-capped Au NPs, the aqueous TBA solution (20 mL, 2–20 mM) was added to the boiling solution of $HAuCl_4$ (50 mL, 0.2 mM) under vigorous stirring in a round bottom flask equipped with a condenser. On addition of TBA to tetrachloroauric acid solution a transition in color of the reaction mixture was observed from red to colorless within 10 s. The reaction mixture was further boiled for 30 min under reflux and then cooled with stirring to room temperature i.e. 25 °C. The pH of the TBA-capped Au NPs solutions was adjusted to desired pH 5–8 with 0.1 M NaOH solution.

2.3. Characterization technique

Optical absorption measurements were performed using (Perkin-Elmer Lambda 750) UV–vis-NIR spectrophotometer. The particle size and morphology of the NPs were examined using transmission electron microscope (FEI Tecnai G20) operated at an accelerating voltage of 220 keV. All the samples for transmission electron

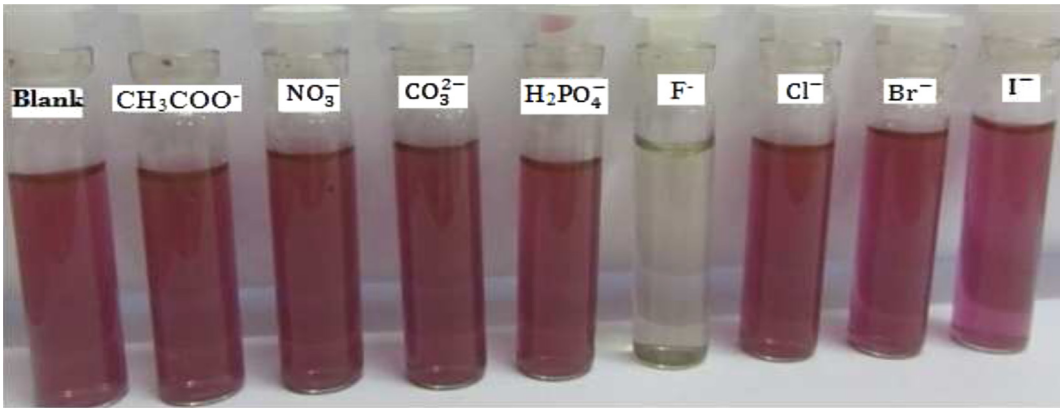

Fig. 3. Color changes of the 2-thiobarbituric-capped gold nanoparticles having 10 mM concentration in the presence of 10 mM anions concentration.

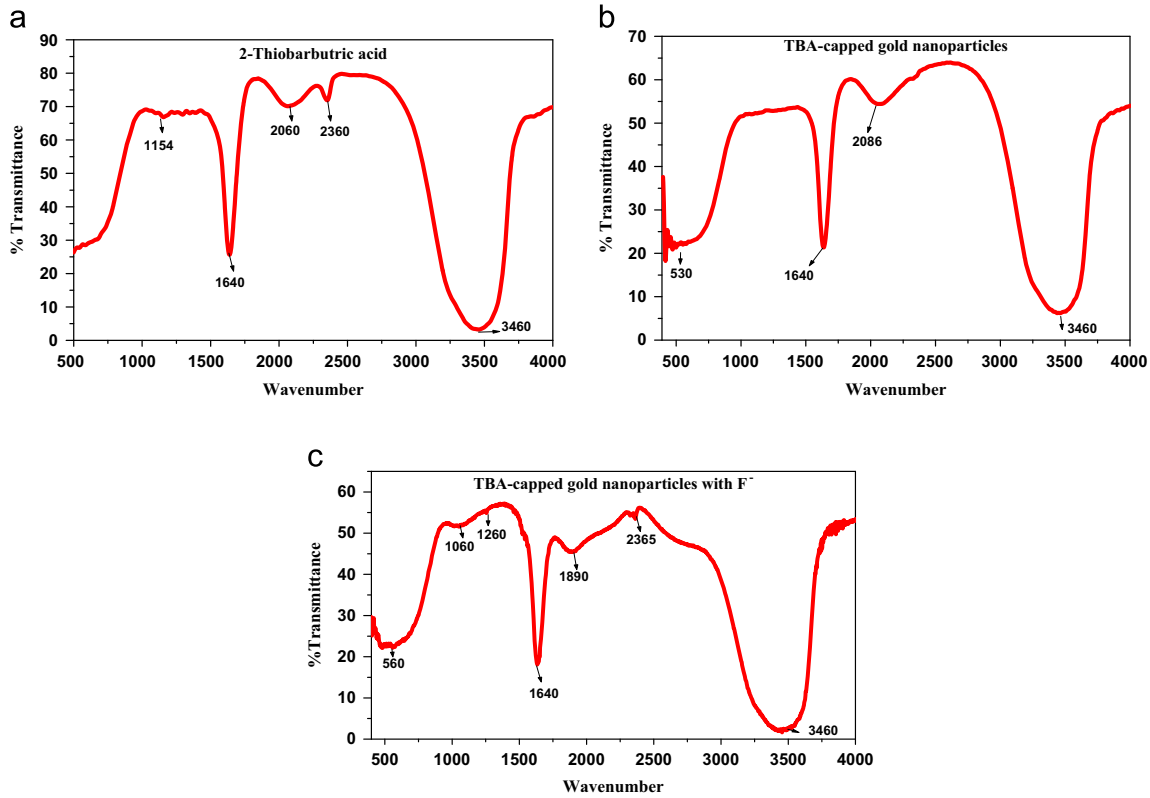

Fig. 4. FTIR spectra of (a) 2-thiobarbituric acid (b) 2-thiobarbituric-capped gold nanoparticles and (c) TBA-capped gold nanoparticles with fluoride ion.

microscope (TEM) were deposited on carbon coated copper grid by placing the drops of diluted samples of TBA-capped Au NPs. Fourier transformation infrared (FTIR) spectrometer (Agilent Cary 660, USA) and Raman spectrometer (Deltanu Advantage 532) were used to obtain information of an element to element bonding or interaction.

3. Results and discussion

The absorption spectrum of Au NPs showed the maximum peak at 554 nm attributed to the localized surface plasmon resonance (LSPR) band. The thiol group is essential to synthesize well dispersed TBA-capped Au NPs. In the synthesis of TBA-capped AuNPs, the position of thiol group plays an important role in the reaction mixture. The analytical method developed herein is novel, rapid, very simple and highly selective which involves the use of sodium fluoride in the presence of TBA-capped Au NPs for the visual detection of hazardous fluoride ion.

3.1. TBA-capped Au NPs fluoride interaction

A schematic representation of synthesis of TBA-capped Au NPs and its interaction with fluoride ion is shown in Fig. 1. The typical LSPR absorbance band of TBA-capped Au NPs at 554 nm provided red color in the absence of fluoride ion and the solution was stable under the experimental conditions. When the fluoride was added to TBA-capped Au NPs solutions, the color dramatically changed from red to colorless and the absorption bands were red shifted i.e. at longer wave length within mixtures which indicated the aggregation of TBA-capped Au NPs [65]. The color transformation was completed within 40 s. On the other hand, other anions did not induce any color change at 10 mM concentration. The UV–vis spectra of the reaction mixture remained unchanged in the presence of fluoride ion over several hours. This observation concluded the formation of H–F hydrogen bonding in the reaction mixture of TBA-capped Au NPs and fluoride ion. It may be attributed to the high charge density and small size of fluoride ion which enabled the formation of hydrogen bonding by interaction with the hydroxyl groups of TBA moieties (Fig. 1). The color change occurred in the reaction was easily monitored by the naked eye.

3.2. Morphological study of TBA-capped Au NPs

The morphology of the TBA-capped Au NPs was studied using TEM images. Fig. 2 shows a typical TEM image of TBA-capped Au NPs. The shape of the gold nanoparticle was slightly irregular. The average particle size (68–74 nm) can be tuned over a size range of 1–20 nm by varying the concentration of TBA in the reaction mixture.

3.3. Visual color change studies

The sensing of halide anions such as F^-, Cl^-, Br^-, I^- and oxo anions such as CH_3COO^-, NO_3^-, CO_3^{2-}, $H_2PO_4^-$ was studied using UV–vis spectroscopy in aqueous solution. The effect of the addition of these anions to TBA-capped Au NPs solutions is shown in Fig. 3 as photographic images which clearly shows that the color changes only after the addition of F^- (10 mM) to the solution and causes a red shift in the LSPR band. It is remarkable to note that the color changes occurred only when F^- was added while of addition other anions such as CH_3COO^-, NO_3^-, CO_3^{2-}, $H_2PO_4^-$, Cl^-, Br^- and I^- failed to cause any significant change in color. This study confirmed that the addition of 10 mM of fluoride ion solution induces the appearance of color change in the reaction mixture.

3.4. FTIR study of TBA-capped Au NPs

Fourier transformation infrared spectroscopy (FTIR) was performed to find the fluoride binding with TBA-capped Au NPs in the samples and related infrared spectra are shown in Fig. 4(a, b and c). The FTIR spectrum for the Au NPs was compared with corresponding surfactant i.e. TBA and it was found that the S-H stretching frequency (2360 cm^{-1}) of bound surfactants disappeared (Fig. 4a and b). This suggests that the bonding of the thiobarbituric to the gold surface takes place through the S-H end. Further the S-H bond cleaved upon S-Au chemisorption is in good agreement with the study done by Hasan et al. on the fate of sulfur bound hydrogen during the formation of a thiol monolayer on gold [66]. The S-H absorption is typically weak and occurs at a lower wave number (frequency) than the corresponding O-H vibration because of the higher atomic mass of sulfur [67]. Due to a high atomic number of gold its vibrational feature is also expected to appear at lower wave number and appeared at 530 cm^{-1} (Fig. 4b) [68]. The appearance of a new weak band at 2365 cm^{-1} (Fig. 4c) was assigned to the H—F hydrogen bond formation in fluoride ion treated TBA-capped Au NPs solution [67]. It may be due to the weak interaction of fluoride ion with hydroxyl group of TBA as shown in Fig. 1. It was found that the band at 1640 cm^{-1} remained unchanged in all the cases which is consistent with the greater affinity of Au for S-H bond compared with C=N. This observation was consistent with earlier reports that the rigid chain conformation on the nanoparticle surface generates

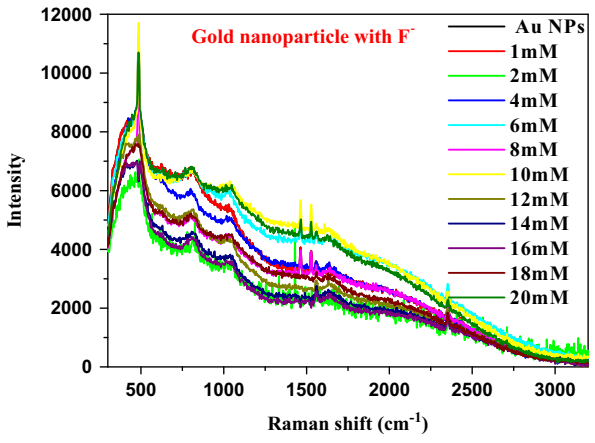

Fig. 5. Raman spectra of 2-thiobarbituric-capped gold nanoparticle with the addition of 1–20 mM of NaF.

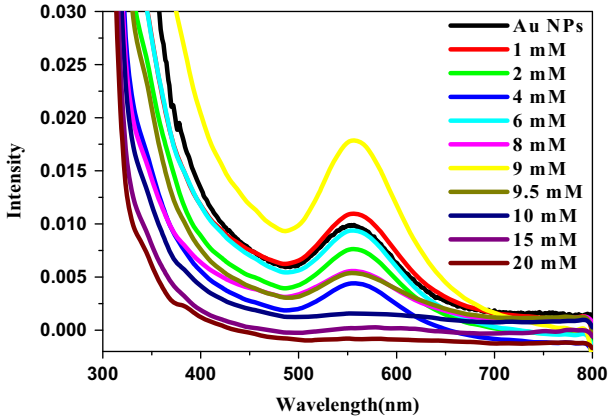

Fig. 6. UV–vis spectra of 2-thiobarbituric-capped gold nanoparticles solution having 10 mM concentration with the addition of different fluoride ion concentrations in the range 1–20 mM in the solution.

a crystalline-like state of chains and restricted their mobility [69]. The band at 3460 cm^{-1} appeared due to O-H stretching present in TBA moieties, which remained same in all the spectra [70].

3.5. Raman spectroscopy study of TBA-capped Au NPs

The Raman spectroscopy has frequently been used to detect vibrations in molecules based on the processes of infrared absorption and Raman scattering which provides information on chemical structure. Raman spectra of TBA-capped Au NPs in presence of different concentration of F^- (1–20 mm) are shown in Fig. 5 which are dominated by the bands around 1030 cm^{-1} and 1530 cm^{-1} attributed to C-S and C-C stretching vibrations respectively. The behavior of other peaks in Raman spectra is consistent with colloidal states [71]. The S-H stretching at 2580 cm^{-1} and S-H bending at 917 cm^{-1} in the Raman spectrum disappeared, indicating dissociative chemisorption of TBA onto Au by rupturing S-H bond [72]. The appearance of a sharp peak at 1470 cm^{-1} evidenced the formation of Au-S bond. These features generally appeared in Raman spectra of thiol [73].

3.6. Sensing assay of fluoride ion

To verify practicality, the proposed method was applied to detect the fluoride ion on the aggregation of Au NPs. 1 mL portion of different concentrations (1–20 mM) of fluoride ion were added individually to 2 mL of TBA-capped Au NPs solutions. The resulting mixtures were allowed to react for 1–5 min. The absorption changes between 550–700 nm were monitored. The extinction at a wavelength above 600 nm was similar to the collective plasmon resonance of closely spaced Au NPs which indicated the anion i.e. F^- induced aggregation of NPs. At certain threshold concentration

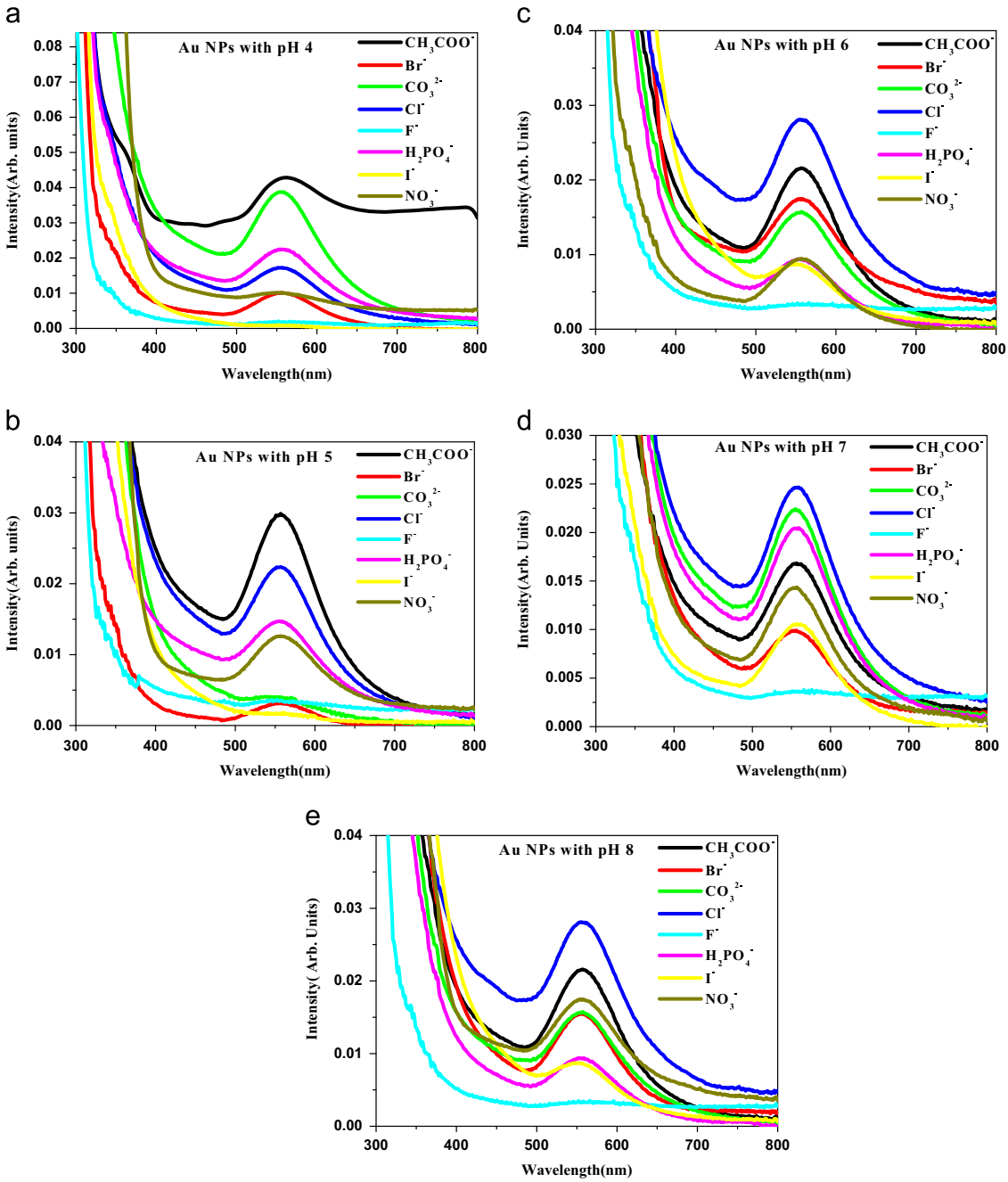

Fig. 7. UV–vis spectra of TBA–capped Au NPs solution having 10 mM concentration at different pH: (a) pH 4, (b) pH 5, (c) pH 6, (d) pH 7 and (e) pH 8.

of F^-, difference in the concentration can be detected by the naked-eye as the color change from red to colorless [35].

The UV–vis spectra of TBA-capped Au NPs solution upon addition of increasing fluoride ion concentrations in the range of 1–20 mM is shown in Fig. 6. Fig. 6 clearly shows that with increasing the amount of fluoride ion in the solution, the intensity of peaks decreased and at the certain concentration peak just disappeared. The peak width was also increased with the addition of higher concentration of fluoride ion in the solution. The changes observed in both parameters revealed the aggregation of NPs [13,65]. The addition of fluoride ion to the TBA-capped Au NPs solution caused dramatic changes in the plasmon band while the interaction was very strong at 10 mM F^- concentration. This concentration displays the colorimetric detection of F^- where the characteristic peak at 554 nm i.e. LSPR disappeared. UV–vis spectra at different concentrations of fluoride showed that with increased concentration of F^- in the reaction mixture, the peak position remained same while decreased in its intensity as well as broadening in the spectra occurred.

3.7. Effect of pH and TEM study

To investigate the effect of pH on the aggregation, the pH of TBA-capped Au NPs solution was varied by using 0.1 M NaOH from 4 to 8 [74]. The UV–vis spectra in the presence of different anions, obtained at different pH, are shown in Fig. 7 (a-e). With increasing pH i.e. increasing density of OH^- in the solution, the nucleophilicity of F^- increased to bind with protective surface of NPs. This result also indicates that the sensing process of F^- is govern by hydrogen bonding and by adsorption phenomenon, otherwise at pH 8, I^- ions could have also bonded with the hydrogen of capping agent i.e. TBA. With an increasing pH of the solution, the efficiency of interaction of larger anions decreases due to their decreased interaction [75]. At pH 8 almost all anions were stable due to their larger size while smaller F^- has strong tendency to disperse its excess charge through the formation of hydrogen bond with the capping agent. This study concluded that the selectivity of F^- ion detection increased with increasing pH of the solution.

The variation of pH from 4 to 8 of Au NPs did not show any change in the red color of the solution which confirmed the stability of the disperse state of TBA-capped Au NPs in the studied pH range. Initially, the pH of TBA-capped Au NPs solution was monitored to be around 2.7–3.0. On decreasing the pH of the solution, the position of the absorption peak remained same while changes observed in their shape and intensity. Very low pH decreases the electrostatic stability of Au NPs by decreasing hydroxyl (–OH) group concentration. The low intensity as well as very broad peaks indicated that the number of Au NPs at the surface significantly decreased by the aggregation of Au NPs or due to decrease in particle to particle distance.

The aggregation of Au NPs at pH 5 to 8 was further confirmed by TEM analysis. The TEM micrographs of Au NPs solution at pH 5, 6, 7 and 8 are shown in Fig. 8(a-d) which clearly show high aggregation at pH 5 and least at pH 8. The TEM images of Au NPs at various pH show that the aggregation occurs maximum at pH 5 while the particles are still dispersed without signs of aggregation at pH 6–8. The maximum aggregation at pH 5 is attributed to the fact that aggregation takes place due to the closer confinement of the particles [65]. TEM images of TBA-capped Au NPs after addition of fluoride ion indicate the formation of aggregated Au

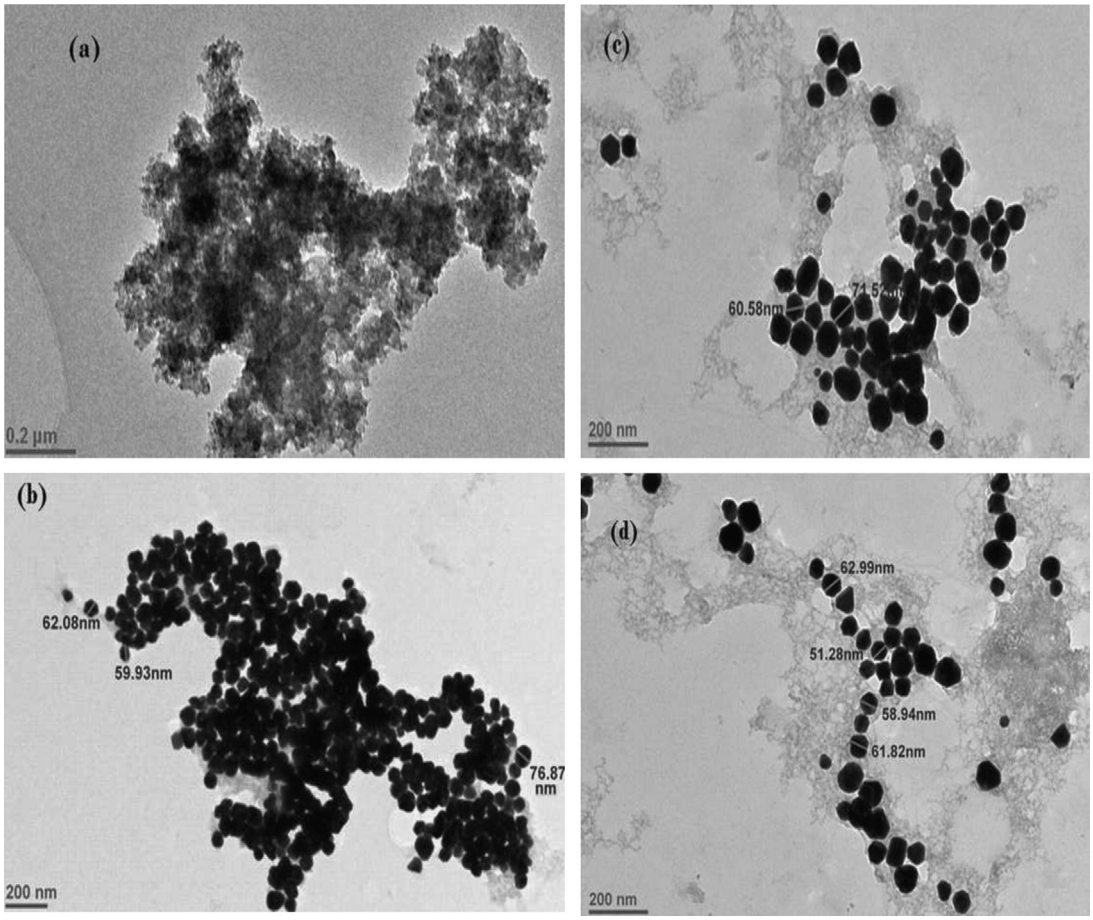

Fig. 8. Transmission electron microscope images of gold nanoparticles at different pH: (a) pH 5, (b) pH 6, (c) pH 7 and (d) pH 8.

NPs as shown in Fig. 8(a). This is attributed to the reduction of interparticle distance. When the distance among the aggregated particles decreases to less than the average particle diameter, the electric dipole-dipole interaction and coupling between the Plasmon's of neighboring particles into the aggregates leads to the formation of a new absorption band at longer wavelengths i.e. red shift the same was observed in Section 3.1 [65,76,77] while the broadening is attributed the slow rate of interaction [65,77].

4. Conclusions

In summary, we have demonstrated a simple way for the development of TBA-capped Au NPs by the chemical reduction method and used as platform for the detection of fluoride ion. In aqueous solution, halide anions (except fluoride) and oxoanions did not induce the aggregation with TBA-capped Au NPs. The color change associated with F^- aggregation has successfully been used for the naked eye detection of F^- at 10 mM concentration in aqueous solution. The reaction of F^- with TBA-capped Au NPs in aqueous solution has also been confirmed by Raman and FTIR spectroscopy.

Acknowledgments

J. Boken is thankful to the Department of Science and Technology (DST), Government of India, New Delhi for financial assistance via grant no. F.No.SR/WOS-A/PS-35/2010. The authors are thankful to Professor Aditya Shastri, Vice Chancellor, Banasthali University, Banasthali for kindly extending the facilities of 'Banasthali Centre for Education and Research in Basic Sciences' sanctioned under CURIE programme of the DST, Government of India, New Delhi, India.

References

[1] Z. Altintas, S.S. Kallempudi, Y. Gurbuz, Talanta 118 (2014) 270–276.
[2] R. Domínguez-González, L.G. Varela, P. Bermejo-Barrera, Talanta 118 (2014) 262–269.
[3] C.L. Haynes, R.P. Van Duyne, Phys. Chem. B 105 (2001) 5599–5611.
[4] R.C. Jin, Y.W. Cao, C.A. Mirkin, K.L. Kelly, G.C. Schatz, J.G. Zheng, Science 294 (2001) 1901–1903.
[5] R. Jin, Y.C. Cao, E. Hao, G.S. Metraux, G.C. Schatz, C.A. Mirkin, Nature 425 (2003) 487–490.
[6] A.D. McFarland, R.P.V Duyne, Nano Lett. 3 (2003) 1057–1062.
[7] J.J. Mock, D.R. Smith, S. Schultz, Nano Lett. 3 (2003) 485–491.
[8] M.D. Malinsky, K.L. Kelly, G.C. Schatz, R.P. Van Duyne, J. Am. Chem. Soc. 123 (2001) 1471–1482.
[9] W.A. Murray, B. Auguie, W.L. Barnes, Phys. Chem. C 113 (2009) 5120–5125.
[10] M.M. Maye, L. Han, N.N. Kariuki, N.K. Ly, W.B. Chan, J. Luo, C.J. Zhong, Anal. Chim. Acta 496 (2003) 17–27.
[11] I. Hussain, M. Brust, A.J. Papworth, A.I. Cooper, Langmuir 19 (2003) 4831–4835.
[12] L. Zhao, K.L. Kelly, G.C. Schatz, Phys. Chem. B 107 (2003) 7343–7350.
[13] A.A. Lazarides, K.L. Kelly, T.R. Jensen, G.C. Schatz, J. Mol. Str. Theochem 529 (2000) 59–63.
[14] Meenakshi, R.C. Maheshwari, J. Hazar. Mat. 137 (2006) 456–463.
[15] V. Tomar, S. Prasad, D. Kumar, Microchem. J. 111 (2013) 116–124 (and references cited therein).
[16] V. Tomar, S. Prasad, D. Kumar, Microchem. J. 112 (2014) 97–103 (and references cited therein).
[17] S. Thatai, P. Khurana, S. Prasad, D. Kumar, Microchim. J. 113 (2014) 77–82 (and references cited therein).
[18] P. Singh, M.K. Barajatiya, S. Dhing, R. Bhatnagar, S. Kothari, V. Dhar, Urol. Res. 29 (2001) 238–244.
[19] G.E.J. Poinern, M.K. Ghosh, Y.-J. Ng, T.B. Issa, S. Anand, P. Singh, J. Hazar. Mat 185 (2011) 29–37.
[20] J.M. Kauffman, J. Am. Phys. Surg. 10 (2005) 38–44.
[21] S.O. Obare, R.E. Hollwell, C.J. Murphy, Langmuir 18 (2002) 10407–10410.
[22] S.Y. Lin, S.W. Liu, C.M. Lin, C.H. Chen, Anal. Chem. 74 (2002) 330–335.
[23] J. Liu, Y. Lu, Fluorescence 14 (2004) 343–354.
[24] N. Kumari, N. Dey, S. Bhattacharya, Analyst 139 (2014) 2370–2378.
[25] Y. Kubo, S. Uchida, Y. Kemmochib, T. Okubob, Tetrahedron Lett. 46 (2005) 4369–4372.
[26] A. Pandya, K.V. Joshi, N.R. Modi, S.K. Menon, Sensor Actuator B 168 (2012) 54–61.
[27] W.L. Daniel, M.S. Han, J.S. Lee, C.A. Mirkin, J. Am. Chem. Soc. 131 (2009) 6362–6363.
[28] L. Xiong, J. Feng, R. Hu, S. Wang, S. Li, Y. Li, G. Yang, Anal. Chem. 85 (2013) 4113–4119.
[29] Z.H. Lin, S.J. Ou, C.Y. Duan, B.G. Zhang, Z.P. Bai, Chem. Commun. 6 (2006) 624–626.
[30] J.A. Gu, Y.J. Lin, Y.M. Chia, H.Y. Lin, Microchim. Acta 180 (2013) 801–806.
[31] F. Du, Y. Bao, B. Liu, J. Tian, Q. Li, R. Bai, Chem. Commun. 49 (2013) 4631–4633.
[32] D.A. Jose, D.K. Kumar, B. Ganguly, A. Das, Org. Lett. 6 (2004) 3445–3448.
[33] A. Satheshkumar, E.H. El-Mossalamy, R. Manivannan, C. Parthiban, L.M. Al-Harbi, S. Kosa, K.P. Elango, Spectrochim. Acta A 128 (2014) 798–805.
[34] A.B. Sarıgüney, A.Ö. Saf, A. Coşkun, Spectrochim. Acta A 128 (2014) 575–582.
[35] S. Watanabe, H. Seguchi, K. Yoshida, K. Kifune, T. Tadaki, H. Shiozaki, Tetrahedron Lett. 46 (2005) 8827–8829.
[36] J.M. Liu, L.P. Lin, X.X. Wang, L. Jiao, M.L. Cui, S.L. Jiang, W.L. Cai, L.H. Zhang Z.Y. Zheng, Analyst 138 (2013) 278–283.
[37] S.Y. Kim, J. Park, M. Koh, S.B. Park, J.I. Hong, Chem. Commun. (2009) 4735–4737.
[38] S.S.R. Dasary, P.C. Ray, A.K. Singh, T. Arbneshi, H. Yu, D. Senapati, Analyst 138 (2013) 1195-1203.
[39] H. Li, L. Rothberg, Proc. Natl. Acad. Sci. USA 101 (2004) 14036–14039.
[40] V. Kattumuri, M. Chandrasekhar, S. Guha, K. Raghuraman, K.V. Katti, K. Ghosh, R.J. Patel, App. Phys. Lett. 88 (2006) 153114.
[41] S. Rho, S.J. Kim, S.C. Lee, J.H. Chang, H.G. Kang, J. Choi, Curr. App. Phys. 9 (2008) 534–537.
[42] D.J. Maxwell, J.R. Taylor, S. Nie, J. Am. Chem. Soc. 124 (2002) 9606–9612.
[43] Z.S. Wu, S.B. Zhang, M.M. Guo, C.R. Chen, G.L. Shen, R.Q. Yu, Anal. Chim. Acta 584 (2007) 122–128.
[44] A.L. Simonian, T.A. Good, S.S. Wang, J.R. Wild, Anal. Chim. Acta 534 (2005) 69–77.
[45] N. Nerambourg, R. Praho, M.H.V. Werts, D. Thmas, M.B. Desce, Int. J. Nanotech. 5 (2008) 722–740.
[46] X. Zhou, B. Yu, Y. Guo, X. Tang, H. Zhang, W. Liu, Inorg. Chem. 49 (2010) 4002–4007.
[47] S. Mizukami, S. Okada, S. Kimura, K. Kikuchi, Inorg. Chem. 48 (2009) 7630–7638.
[48] H.G. Lee, K.B. Kim, G.J. Park, Y.J. Na, H.Y. Jo, S.A. Lee, C. Kim, Inorg. Chem. Commun. 39 (2014) 61–65.
[49] L.N. Neupane, J.Y. Park, J.H. Park, K.H. Lee, Org. Lett. 15 (2013) 254–257.
[50] M. Seydack, Biosens. Bioelectron. 20 (2005) 2454–2469.
[51] Q. Qian, J. Deng, D. Wang, L. Yang, P. Yu, L. Mao, Anal. Chem. 84 (2012) 9579–9584.
[52] V.M. Chauhan, R.H. Hopper, S.Z. Ali, E.M. King, F. Udrea, C.H. Oxley, J.W. Aylott, Sensor Actuator B 192 (2014) 126–133.
[53] D.A. Pearce, N. Jotterand, I.S. Carrico, B. Imperiali, J. Am. Chem. Soc. 123 (2001) 5160–5161.
[54] T. Hirano, K. Kikuchi, Y. Urano, T. Nagano, J. Am. Chem. Soc. 124 (2002) 6555–6562.
[55] K. Komatsu, K. Kikuchi, H. Kojima, Y. Urano, T. Nagano, J. Am. Chem. Soc. 127 (2005) 10197–10204.
[56] S. Schutting, S.M. Borisov, I. Klimant, Anal. Chem. 85 (2013) 3271–3279.
[57] T. Ghosh, B.G. Maiya, J. Chem. Sci. 116 (2004) 17–20.
[58] C.B. Black, B. Andrioletti, A.C. Try, C. Ruiperez, J.L. Sessler, J. Am. Chem. Soc. 121 (1999) 10438–10439.
[59] T. Mizuno, W.H. Wei, L.R. Eller, J.L. Sessler, J. Am. Chem. Soc. 124 (2002) 1134–1135.
[60] D.H. Lee, K.H. Lee, J.I. Hong, Org. Lett. 3 (2001) 5–8.
[61] K.H. Lee, H.Y. Lee, D.H. Lee, J.I. Hong, Tetrahedron Lett. 42 (2001) 5447–5449.
[62] F.M. Hinterholzinger, B. Ruhle, S. Wuttke, K. Karaghiospff, T. Bein, Sci. Rep. 3 (2013) 2562.
[63] A. Sugunan, C. Thanachayanont, J. Dutta, J.G. Hiborn, Sci. Technol. Adv. Mater. 6 (2005) 335–340.
[64] J. Turkevich, P.C. Stevenson, J. Hillier, Discuss. Faraday Soc. 11 (1951) 55–75.
[65] N.T.K. Thanh, Z. Rosenzweig, Anal. Chem. 74 (2002) 1624–1628.
[66] M. Hasan, D. Bethell, M. Brust, J. Am. Chem. Soc. 124 (2002) 1132–1133.
[67] L. Andrews, S.R. Davis, J. Chem. Phys. 83 (1985) 4983.
[68] I.R. Moraes, M.C.P.M. daCunha, F.C. Nart, J. Braz. Chem. Soc. 7 (1996) 453–460.
[69] P. Pandey, S.P. Singh, S.K. Arya, V. Gupta, M. Dutta, S. Singh, B.D. Malhotra, Langmuir 23 (2007) 3333–3337.
[70] U.J. Kim, C.A. Furtado, X. Liu, G. Chen, P.C. Eklund, J. Am. Chem. Soc. 127 (2005) 15437–15445.
[71] S.W. Han, S.J. Lee, K. Kim, Langmuir 17 (2001) 6981–6987.
[72] H.Y. Jung, Y.K. Park, S. Park, S.K. Kim, Anal. Chim. Acta 602 (2007) 236–243.
[73] D. Maniu, V. Chis, M. Baia, F. Toderas, S. Astilean, J. Optoelectron. Adv. Mater. 9 (2007) 733–736.
[74] E. Carbonell, E. Delgado-Pinar, J. Pitarch-Jarque, J. Alarcón, E. García-España J. Phys. Chem. C 117 (2013) 14325–14331.
[75] G. Zhou, C. Zhao, C. Pan, F. Li, Anal. Methods 5 (2013) 2188–2192.
[76] A. Mocanu, I. Cernica, G. Tomoaia, L.D Bobos, O. Horovitz, M.T. Cotisel, Colloid Surf. A 338 (2009) 93–101.
[77] A.A. Abo-Alhasan, S.A. El-Daly, M.M. El-Hendawy, S.H. El-Khalfy, M.E. El-Zeiny, J. Nanomater. Mol. Nanotechnol. 3 (2014) 1–7.